J Mater Sci (2011) 46:1963–1974
DOI 10.1007/s10853-010-5032-0

Ductile-*to*-brittle transition in cenosphere-filled polypropylene composites

Bhabani K. Satapathy · Arijit Das · Amar Patnaik

Received: 22 July 2010 / Accepted: 25 October 2010 / Published online: 16 November 2010

Abstract Cenosphere-filled polypropylene (PP) composites were fabricated and characterized for their structural/morphological and fracture mechanical behaviour. The fracture properties were studied following the essential work of fracture (EWF) approach based on post-yield fracture mechanics (PYFM) concept. The structural attributes and its consequent effects on the dynamic mechanical properties were characterized by wide angle X-ray diffraction (WAXD), hot-stage polarized light optical microscopy (PLOM) and dynamic mechanical analysis (DMA). The WAXD studies have revealed a decrease in crystallinity of the composites with increase in cenosphere content. PLOM studies reveals a threefold reduction in the diameter of the spherulite in case of composite with 10 wt% of cenosphere compared to that of PP followed by an increase of $\sim$50% in the composite with 20 wt% of cenosphere compared to that of the composite with 10 wt% cenosphere. DMA revealed an enhancement in the energy dissipation ability of the composite with 10 wt% of cenosphere and an increase in the storage modulus up to $\sim$30% in the composites relative to the soft PP phase. The non-essential work of fracture (NEWF: βw_p) as the resistance to stable crack propagation has shown a maximum at 10 wt% of cenosphere followed by a sharp drop at higher cenosphere content indicating a cenosphere-induced ductile-*to*-brittle transition (DBT). Fractured surface morphology investigations revealed that the failure mode of the composites undergo a systematic transition from matrix-controlled shear deformation to filler-controlled quasi-brittle modes above a cenosphere loading of 10 wt% in the composites reiterating the possibility of filler-induced semiductile-*to*-DBT transition.

B. K. Satapathy (✉) · A. Das
Centre for Polymer Science and Engineering, Indian Institute of Technology Delhi, Hauz Khas, New Delhi 110016, India
e-mail: bhabaniks@gmail.com

A. Patnaik
Department of Mechanical Engineering, National Institute of Technology, Hamirpur 177005, India

Introduction

Tough polypropylene (PP) has an attractive price and exhibits good mechanical properties and thermal resistance. However, the moderate fracture performance, especially at sub-ambient temperatures, has always been an obstacle for both engineering and less demanding commodity and structural applications. Conventionally, the low-temperature impact resistance of PP is usually improved by melt blending (incorporation of various elastomers into PP) or by copolymerization techniques (via in situ formation of a dispersed elastomer phase within the PP matrix), though such an advantage is met at the cost of material modulus (E) and strength (σ_y). Typically, to improve the stiffness-*to*-toughness balance of elastomer-toughened PP, fillers (e.g. talc, calcium carbonate) or reinforcing fibres (e.g. short glass fibres) are added. Rigid and hollow spherical fillers such as glass beads or flyash-derived cenospheres also prove to be effective in enhancing the stiffness. Interestingly, the regular spherical shape of such potential fillers make them an excellent choice since the mechanical response of their composites are expected to be isotropic and thereby making them suitable systems for modeling and theoretical studies. However, poor incompatibility between the hydrophobic polymer and hydrophilic flyash (FA) cenospheres may lead to inferior interfacial adhesion causing inappreciable performance benefits. In contrast, the hydroxyl groups on flyash (FA)

cenosphere surface may cause cluster or agglomeration tendency between themselves leading to strong filler–filler interaction in the matrices, a situation causing non-uniform macroscale distributions consequentially giving rise to mechanical anisotropy [1–3].

Therefore, flyash–flyash–cenosphere-filled polymer composites have been extensively investigated concerning effects of particle size and surface treatments of filled polyesters [4], correlation of structural and mechanical properties of filled isotactic PP [5], solvent resistance and weather resistance of filled unsaturated polyesters [6], the selective response to several tribological situations such as two-body abrasion [7], three-body abrasion [8], erosion [9] and friction braking [10], damping properties of filled epoxy [11–13], effects of multi-component compounding [14], conductivity of poly-pyrrole-based composites [15] and compressive and ultrasonic properties of filled polyesters [16]. In addition, the microstructural interpretations of flyash/cenosphere-based composites under uniaxial tensile loading have conventionally been greatly emphasized [17–19]. However, the pragmatic performance evaluation of cenosphere- or flyash-filled composites, before their being declared as an alternative material concept for several structural and mechano-functional applications, needs to be critically assessed using fracture mechanics principles to qualitatively/semi-empirically reach at an ideology of enhanced fracture resistance with individual attention to crack initiation and crack propagation phenomena.

In the light of the above, this study makes an attempt to investigate the fracture behaviour of cenosphere-filled PP composites using pre-notched artificially pre-cracked specimens in uniaxial tension mode following the essential work of fracture (EWF) approach based on post-yield fracture mechanics (PYFM) concept. The method theoretically enables the separation of the two energy related terms corresponding to crack initiation in the inner fracture process zone and crack propagation in the outer plastic deformation zones. Mechanistically, the two stages of crack growth, i.e. initiation and propagation, have a quantitative correspondence to EWF and non-essential work of fracture (NEWF), respectively. The conceptual validity of EWF methodology has already been established in several PP-based homopolymer grades, blends, composites and alloy systems [20–25].

Experimental

Preparation of PP/cenosphere composites

The details of the materials selected and the processing conditions are given in Tables 1, 2, 3, and 4. The mixing of the two ingredients for the fabrication of the composites was carried out in a counter-rotating-type (S.K. Dey Make-2008) twin-screw extruder. The counter-rotating-type twin-screw extruder was used instead of the conventionally used co-rotating twin screw extruder to facilitate the slippage of cenospheres against each other in the melt and thereby assisting in the process of aggregates break-up and better dispersive mixing. The continuous strands thus obtained were later chopped in a granulator and subsequently kept

Table 2 Extrusion temperature profile

Zones	Z-1	Z-2	Z-3	Z-4
Temperature (°C)	190	210	230	240

Table 3 Temperature profile set in injection molding machine

Zones	Feed	Z-1	Z-2	Z-3	Z-4
Temperature (°C)	35	175	185	200	220

Table 4 Processing parameters used in injection molding machine

Process parameters	Values
Injection pressure	5 MPa
Injection speed	30 mm/min
Holding time	14 s
Back pressure	0.5 MPa
Cooling time	18 s

Table 1 Data sheet of raw materials and their characteristics

Raw materials	Grade	Supplier	Characteristics
Polypropylene homopolymer	REPOL H110MA	Reliance Industries Limited	Density (ρ) = 0.91 g/mL; T_m (°C) = 220 °C; MFI (g/10 min) = 11 @ 230 °C, 2.16 kg
Cenosphere	CS-300[a]	Micro Minechem India Pvt. Ltd.	Particle density = 0.45–0.80 g/mL; Particle size = 60–300 μm; Light grey powder; Non-soluble in water; T_m = 1300–1500 °C

[a] The cenospheres are spherical and are free of any surface irregularities which typically occur due to attached tapered/needle/flake-like impurities onto the surface of flyash cenospheres. These irregularities were scrubbed-off to obtain surface irregularity-free hollow microspheres which are referred as cenospheres

Table 5 Details of the composition, designation and crystallinity of the PP–Cenosphere composites

Serial. no.	Composition designation	Polypropylene (wt%)	Cenosphere content (wt%)	Crystallinity[a] (%)
1	PPC-0	100	0	67
2	PPC-5	95	5	59
3	PPC-10	90	10	56
4	PPC-15	85	15	50
5	PPC-20	80	20	49

[a] The crystallinity (%) values of the composites are based on Differential Scanning Calorimetry (DSC) measurements

for drying in the oven before injection molding (L&T Demag make) of the same to obtain plates of 80 mm × 80 mm square plates of 1-mm thickness. Rectangular strips of 80 mm × 20 mm × 1 mm were cut from these plates for fracture mechanical investigations and samples of 35 mm × 15 mm × 1 mm plates were cut for DMA studies. The details of the composite designations are given in Table 5.

Structural characterization/2D wide angle X-ray diffraction (WAXD)

Wide angle X-ray diffraction (WAXD) was carried out on the extruded granules (quasi-isotropic sample) to characterize crystallinity and orientation in the samples, apart from investigating the changes in the peaks corresponding to different crystal planes as a function of cenosphere content. The semi-crystalline PP matrix and cenospheres as Mg–Na–Al mixed silicates having crystal planes as PP lamellae and the silicate planes cause diffraction of X-rays. The measurements were done on an X-pert PRO (Netherland) model-PW 3040-60 X-ray diffractometer of PAN analytical using Ni-filtered Cu Kα radiation of 1.54 Å. The crystallinity was evaluated by applying the peak-area integration method in the range of $2\theta = 10$–$35°$ (as typical for PP) by applying an amorphous scattering curve that was realized by experimental and theoretical experiences.

Polarized light optical microscopy

Polarized light optical microscopy of the pure PP and the cenosphere-filled compositions were carried out on a hot-stage Instec HCS-302 (Meiji Techno-Japan) microscope in a cooling mode to investigate the nature of spherulite growth and the size of the spherulites. The microscope has a camera of 2 mega-pixel resolution with a maximum magnification of 20.

Dynamic mechanical analysis (DMA)

Dynamic mechanical analysis (DMA) measurements have been carried out on the composite test specimens with dimensions of 35 × 15 × 1 mm^3 in tensile mode on a Q800 (TA Instruments, USA) to characterize the storage modulus, loss modulus, and tan δ for qualitatively investigating the reinforcement effects and quantitatively ascertaining shift (if any) in glass transition temperature of the composites in the temperatures ranging between −30 and 165 °C at a frequency of 1.0 rad/s and heating rate of 5 K/min.

Essential work of fracture (EWF) measurements

The EWF was determined using rectangular injection moulded bars of 80 mm × 20 mm × 1 mm dimension which were cut from injection moulded plates of 80 mm × 80 mm × 1 mm dimension. The rectangular bars were cut in such a manner that the injection molding direction and the direction of the application of uniaxial tensile force onto the bars remained identical. The samples were pre-notched with different ligament lengths varying from ~2–9 mm. The fracture of these pre-notched specimens was carried out using a universal tensile testing machine (Zwick Z010) under constant extension speed to obtain individual load–displacement curves. The EWF method has been used since it methodically enables the distinguishing between two terms representing the *resistance to crack initiation* (w_e) and *resistance to crack propagation* (βw_p) corresponding to inner fracture process zone (IFPZ) and outer plastic deformation zone (OPDZ). The applicability of EWF to filled thermoplastic polymer composites, nanostructure polymers and nanocomposites has been well demonstrated in the literature [20, 26–28]. The precondition for the validity of EWF approach has been demonstrated by the self-similarity nature of the load–displacement diagrams of these composites. In this study, the fracture mechanical tests (test speed: 1 mm/min, room temperature) were performed on double-edge-notched tension (DENT) specimen by a universal testing machine with mechanical grips (Z010 Zwick). The clamp distance was 40 mm. For notching, a special device with fresh razor blades (notch tip radius of 0.20 μm) was used to realize that both notches are similar sized. For each material, at

least eight specimens were tested with different ligament lengths between ~2 mm and ~9 mm.

For plane-stress conditions, the total work of fracture W (KJ/m^2) dissipated in a notched specimen can be divided into a component W_e characterizing the IFPZ and another one W_p corresponding to an OPDZ as schematically shown in Fig. 1. Therefore,

$$W = W_e + W_p = w_e \cdot B \cdot l + \beta w_p \cdot B \cdot l^2 \quad (1)$$

where B, l and β are the specimen thickness, the ligament length and the shape factor of the plastic zone, respectively. After dividing W by the ligament (notched) area, i.e. $B.\ l$, the specific work of fracture w is obtained. The relationship may be represented as

$$w = w_e + \beta w_p \cdot l \quad (2)$$

where the quantities, w_e and βw_p, are in N/mm and N/mm^2 units, respectively.

Based on the fact that the intrinsic fracture process takes place in the inner fracture process zone (IFPZ), the term EWF, the essential work of fracture, is experimentally determined by extrapolation of w as a function of l to zero ligament length. For the quantitative determination of these fracture parameters (w_e and βw_p), several similar-sized specimens with different ligament lengths are monotonically loaded to obtain several data points in the plot of w versus l, the intercept and the slope of which give rise to w_e (EWF: resistance to crack initiation) and βw_p (NEWF: resistance to crack propagation).

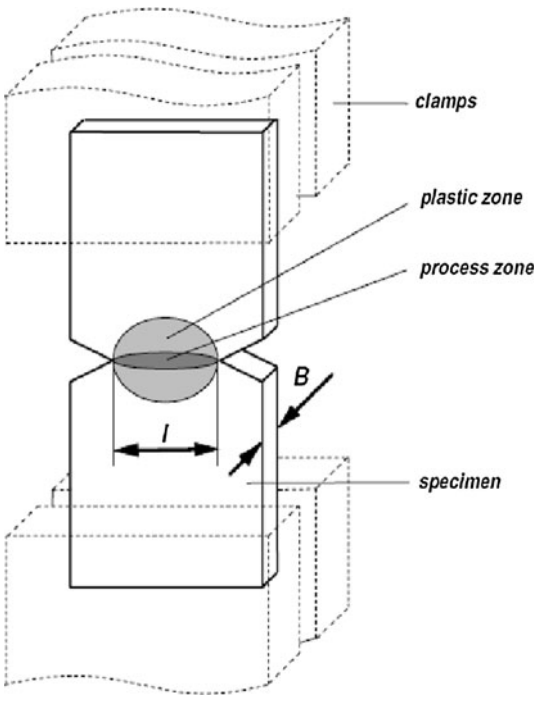

Fig. 1 Double-edge-notched tension (DENT) specimen showing inner fracture process zone (IFPZ) and outer plastic deformation zone (OPDZ)

Fractured surface morphology

The post-yield fractured surface morphologies of virgin PP, cenosphere-filled PP composites, have been investigated using scanning electron microscopy (SEM) on a Zeiss EVO-50 electron microscope to analyse the associated failure mechanisms and structural integrity of such multi-phase microcomposite materials. The surfaces of the specimens were gold sputter coated before examination to make the surfaces conductive.

Results and discussion

Structural characterization by 2D wide angle X-ray diffraction (WAXD)

The structural characteristics of the PP/cenosphere composites have been made from WAXD on extruded granules and SEM studies on cryo-fractured specimen surfaces as has already been reported in previous study by the authors [29]. The uniform distribution/dispersion of cenospheres in the PP matrix of the composites has already been reported therein. The X-ray diffractogram (XRD) plots in terms of I versus 2θ measured in the 2θ range of ~10–35° are shown in Fig. 2. The pure PP is characterized by the intense and prominent peaks assigned as a, b, c, d and e with the peaks a and b being accompanied by low intensity shoulder peaks. The details of Bragg-diffraction angles and the corresponding d-spacing for the various peaks marked in Fig. 2 are given in the figure caption. Interestingly,

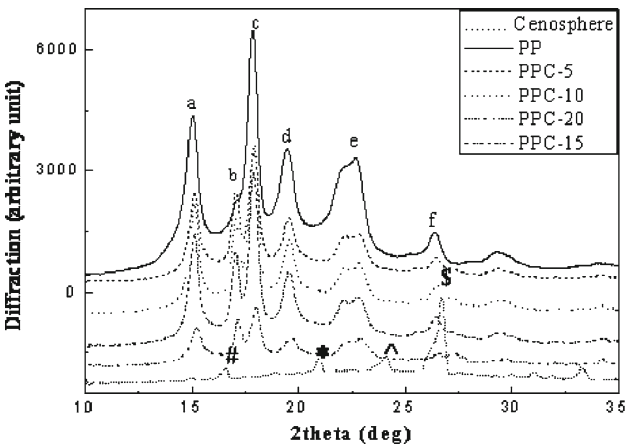

#16.5[°]; 5.37[A°] , *20.7[°]; 4.29[A°] , ^23.9[°]; 3.72[A°], $26.7[°]; 3.34[A°]
a:15.0[°]; 5.92[A°], **b:**17.0[°]; 5.19[A°], **c:**17.8[°]; 4.96[A°], **d:** 19.5[°]; 4.56[A°], **e:**22.8[°]; 3.90[A°], **f:** 26.3[°]; 3.38[A°]

Fig. 2 X-Ray diffractograms (XRD) of PP cenosphere composites

cenosphere is characterized by the peak flanked by the peaks *a* and *b* which are relevant to pure PP. In addition to these peaks, two cenosphere-specific peaks have been observed to be surrounding the peak *d*. The most intense peak of cenosphere has been observed to be overlapping peak *e* of PP. These observations inevitably indicate that the incorporation of cenosphere may have caused structural reorganization of the crystalline regions of PP as inferred from the appearance of distinct peak-splitting of the two intense peaks *b* and *d* accompanied by a reduction in intensity with the increase in cenosphere content. This clearly indicates that the crystalline phase/orientation (of the polymer chains) is appreciably affected due to the cenosphere incorporation though it remained inappreciably influenced by the cenosphere content. Such observations apparently imply the tendency of the crystalline phases for being more disorganized, causing a reduction in the intensity levels [29]. The crystallinity of the various composites as well as that of the virgin PP was determined by area (based on approximation of crystalline and amorphous area) integration technique. The percentage crystallinity systematically decreased with the increase in the cenosphere content as shown in the Table 5. The influence of cenosphere on the variation of crystallinity and its consequent effects on structural, mechanical and micromechanical properties have already been discussed in a previous article by the authors [29].

Polarized light optical microscopy

The polarized light optical microscopy images of the various compositions are shown in Fig. 3. The PLOM of the virgin PP and the composites were carried out on a hot-stage microscope, allowing the hot polymer melt above its melting point (165 °C) and to be slowly cooled down to 120 °C. The cooling down process of the melt enables the growth of the crystalline domains from a purely amorphous melt stage. The photo micrographs revealing the growth of the crystallites units referred as spherulites are shown in Fig. 3. It was observed that in terms of size scale the spherulites suffered a threefold reduction with the incorporation of 10 wt% of cenosphere as compared to that of pure PP. In case of pure PP, the size (diameter) of the spherulite is found to be ~94 μm which decreased to ~36 μm in case of PPC-5 and to a further decreased size of ~30 μm in case of PPC-10. However, on increasing the level of cenosphere loading further into the composites, the spherulites size gradually increased to ~50 μm and ~46 μm for PPC-15 and PPC-20, respectively. This inevitably indicates that the incorporation of alumino-silicate-based rigid hollow microspheres such as cenospheres promotes a faster nucleation. The absence of the peak corresponding to β-PP crystalline phase, as has already been observed from the WAXD plot, further indicates that the cenospheres are strongly α-nucleating [30]. The substantial extent of spherulite size reduction in case of PPC-10 leads to a consequential decrease in the width of the inter-spherulitic grain boundaries [30–32]. Such a decrease contributing to enhanced resistance to crack propagation has been well illustrated in the literature for several other filled polymer systems. Conceptually, smaller spherulites promote faster energy dissipation ability and contribute to deceleration of crack propagation kinetics [33].

Dynamic mechanical analysis

The results from solid state dynamic mechanical response in terms of variation of storage-modulus (E') and loss-modulus (E'') with temperature are shown in Fig. 4a and b and have already been discussed in detail in our earlier published article [29]. The variation of E'' with temperature as shown in Fig. 4b shows that the magnitude of E'' increases substantially with the incorporation of 10 wt% (PPC-10) of cenospheres leading to a maximum, which, however, is followed by a decrease with further increase in cenosphere content. In the entire composition range, E'' remained in between that of the PPC-10 and pure PP. Such a thermo-mechanical response qualitatively indicates the enhancement in the energy dissipation ability of the composite PPC-10. Further, the earlier discussed observation of a threefold reduction in the spherulite size in PPC-10 compared to that of PP additionally supports the possibility of an enhancement in the energy dissipation ability (leading to a maximum in PPC-10) followed by a significant reduction in the composites with a cenosphere content of ≥10 wt%. Thus, it theoretically implies a possible transition in terms of their response to isotropic stress. However, the effect of incorporation of cenosphere has rendered the primary transition temperature of the composites nearly unaffected as revealed from the loss-modulus (E'') curves in Fig. 4b. The combination of high modulus (~13–17 GPa) and microsphere dimensions (~60–300 μm) of cenospheres makes them potentially effective as reinforcement for polymers. The storage modulus (E') versus temperature as plotted in Fig. 4a shows an enhancement of the modulus (with a conceptual correspondence to stiffness) with the increase in the amount of cenosphere, an observation which is well in accordance with theoretical expectation that is typical for rigid spherical particle-filled composites. The extent of increase of storage modulus is relatively high with increasing cenosphere content at lower/sub-zero temperatures i.e. in the range between −25 °C and 0 °C, whereas such an increase is not so pronounced at elevated temperatures. For example, at room temperature, the increase of E' of the composite with 20 wt% cenosphere is ~26% compared to PP matrix

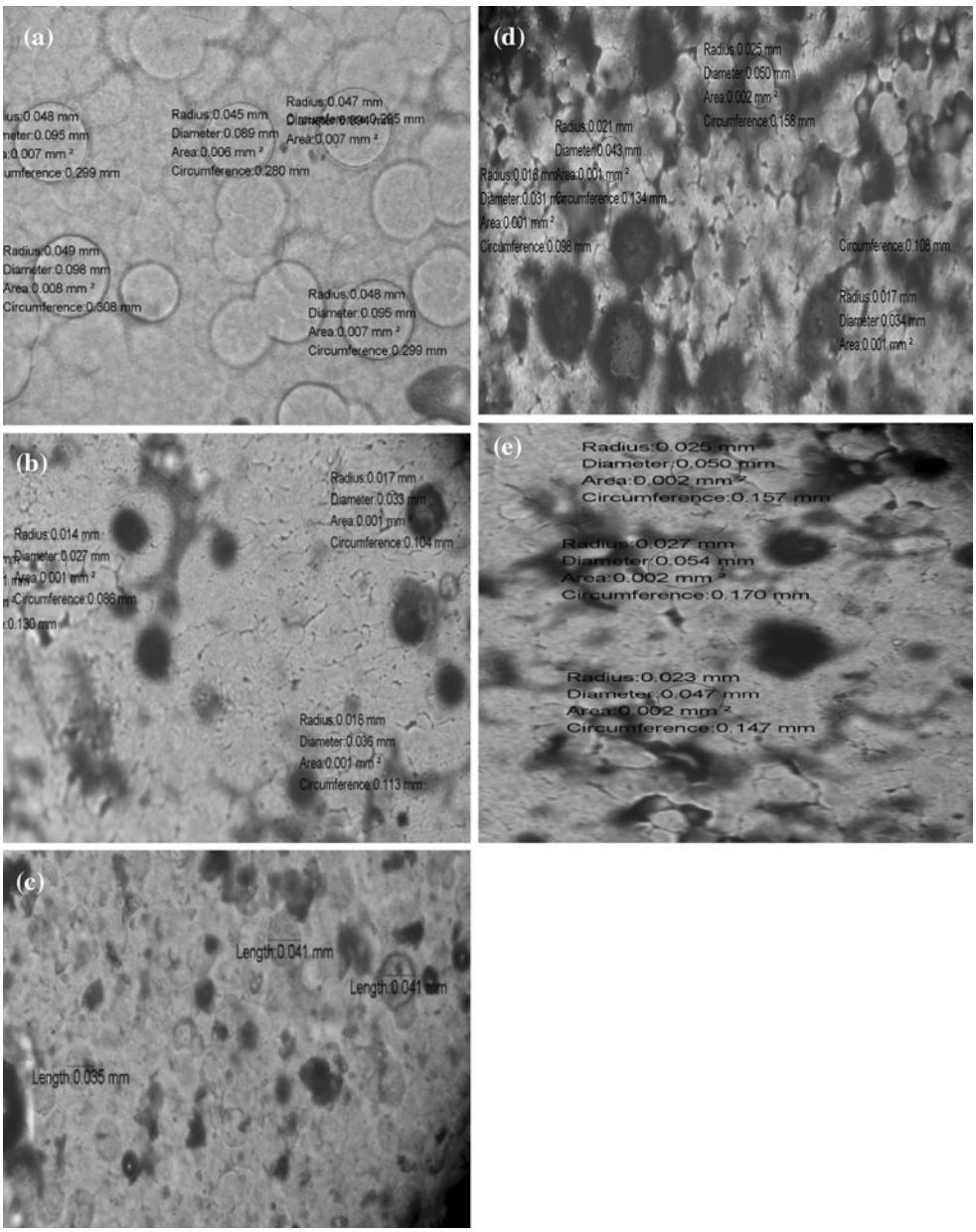

Fig. 3 **a** Polarized light optical microscopy image of PP at a temperature 120 °C. **b** Polarized light optical microscopy image of PPC-5 at a temperature 120 °C. **c** Polarized light optical microscopy image of PPC-10 at a temperature 120 °C. **d** Polarized light optical microscopy image of PPC-15 at a temperature 120 °C. **e** Polarized light optical microscopy image of PPC-20 at a temperature 120 °C

whereas at −10 °C an increase of ∼31% in the E' for the same composition has been observed compared to neat PP.

Fracture behaviour of the microcomposites

Load–displacement diagrams and the validity of EWF approach

In general, PP/cenosphere composites have shown thermoplastic behaviour, and the validity of the EWF methodology through the self-similar nature of the force–displacement curves is shown in Fig. 5a (e.g. PPC15). On the other hand, the plane-stress criterion was confirmed by Hills analysis [27] which revealed that the net section stress remained independent of the ligament length which is shown in Fig. 5b. Full yielding of the ligament in the DENT specimens occurred at maximum load (F_{max}) and before crack propagation started, a pre-conditional aspect for the applicability of EWF principles, which was visually ensured. Clearly, this behaviour observed for these composite systems is well in agreement with conditions for the validity of EWF concept. The method of determination of

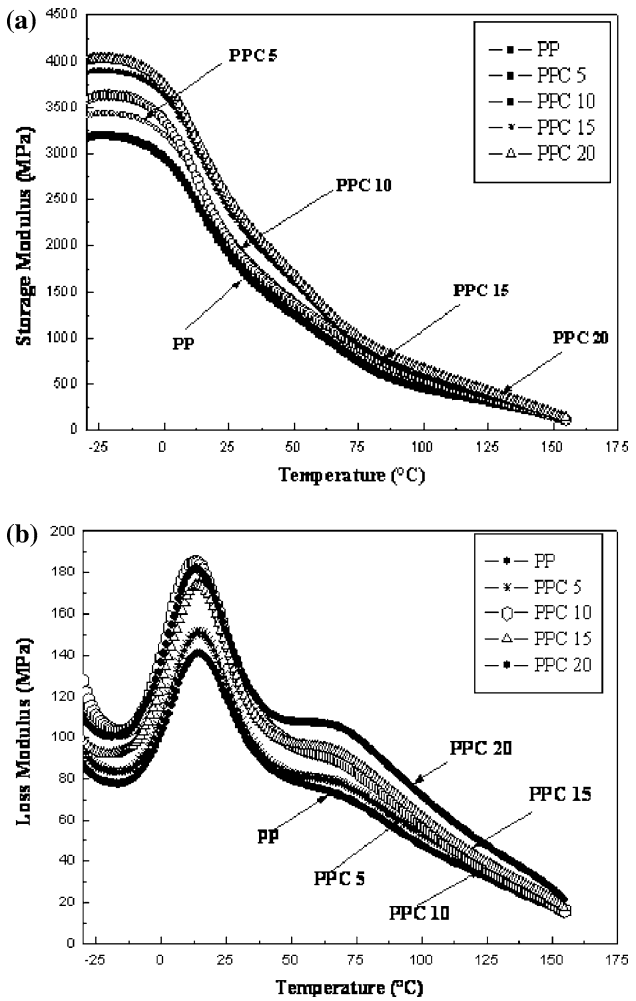

Fig. 4 **a** Dynamic mechanical properties of PP–Cenosphere composites: Storage modulus (E′) as function of temperature; Storage moduli of the various composites @ 30 °C (i) PP = 1740 MPa, (ii) PPC5 = 1986 MPa, (iii) PPC10 = 1879 MPa, (iv) PPC15 = 2216 MPa and (v) PPC20 = 2303 MPa. **b** Dynamic mechanical properties of PP–Cenosphere composites: Loss modulus (E″) as function of temperature

fracture parameters from the plot showing the linear variation of specific work of fracture with ligament length is exemplified for PPC-15 composition in Fig. 5c, where the slope and intercept corresponds to EWF (w_e) and NEWF (βw_p), respectively.

Morphology–work of fracture–toughness correlation

The crack resistance/toughness aspects have been investigated following EWF concept, where EWF: w_e and NEWF: βw_p intrinsically correspond to the resistance against crack initiation and crack propagation, respectively. The conceptual equivalence of J-integral approach to the slope of the linear-fit plot of specific work of fracture against the ligament length representing βw_p has already been demonstrated originally in the literature [28] and in another prominent study by Lach et al. [25]. The equivalence between EWF concept and R-curve concept using the J integral has been shown by Mai and Cotterell [20, 28]. The correlation of PYFM concept to that of the elastic–plastic fracture mechanics (EPFM) concept may be well illustrated as

$$\mathrm{EWF} = J_{\mathrm{Ic}} \tag{1}$$

where the critical J values may be taken as a measure of the stable-crack initiation toughness and

$$\beta w_p = 1/4\ \mathrm{d}J/\mathrm{da}\ (\text{for DENT specimens})$$

where dJ/da is the slope of the J–R curve (a—actual crack length).

Several investigations have led to these findings and confirmed experimentally corresponding to EWF and βwp [34] or numerically (EWF) [35].

The variation in EWF with cenosphere concentration is shown in Fig. 6a. It has been clearly observed that the magnitude of EWF is decreased gradually with addition of cenosphere loading. However, a sharp drop in EWF could be observed on addition of 10 wt% of cenosphere indicating a decreased resistance to crack initiation. The slope of the linear regression fit of the data points in the plot of specific work of fracture versus ligament length represents the NEWF (βw_p) which increases by ~18% on incorporation of 5 wt% of cenosphere as compared to pure PP (Fig. 6b). Interestingly, on further increasing the amount of cenosphere to 10 wt%, βw_p increased sharply when compared to the composite with 5 wt% cenosphere. Quantitatively, the sharp rise in the magnitude of βw_p of the composite with 10 wt% of cenosphere loading was registered to be ~215% when compared to pure PP. However, on further increasing the cenosphere loading in the composites to 20 wt%, the magnitude of βw_p suffered a significant drop, which is almost equivalent to the extent of enhancement at 10 wt% of cenosphere content. The existence of such a non-linear dependence of βw_p on the content of cenosphere indicates a cenosphere-induced ductile-*to*-brittle transition (DBT) in the investigated composites. Qualitatively, the initial enhancement in toughness/resistance to crack propagation till 10 wt% of cenosphere loading in the composites may be attributed to inherent morphological changes/reduction in the size of the crystalline domains (spherulites) as shown in the plot of βw_p versus inverse of spherulite radius (Fig. 7). A direct correlation between toughness as indicated by the magnitude of βw_p and the inverse of spherulite size has been observed that the resistance-*to*-crack propagation may be fundamentally controlled by interfacial effects-assisted crystallization kinetics of PP–cenosphere composites.

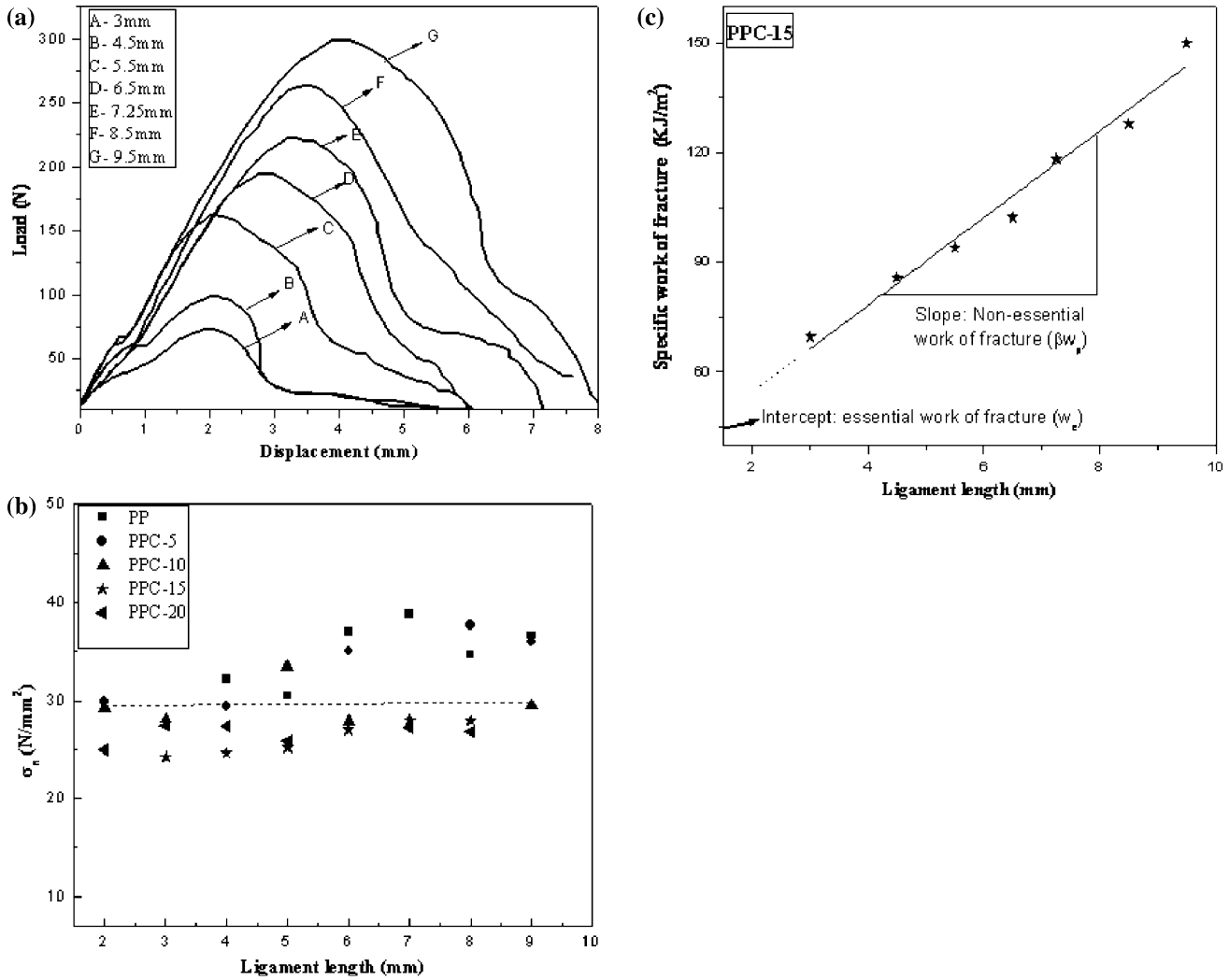

Fig. 5 **a** Self-similarity of Load-displacement diagram as exemplified by PPC-15 for various ligament lengths. **b** Hill's analysis plot: Net section stress versus ligament length. **c** Variation of specific work of fracture with ligament length for PPC-15

Mechanistically, the subsequent drop in the magnitude of βw_p may be attributed to the clustering of the cenosphere particles/filler agglomeration causing weakened interfacial adhesion as has been observed from the fractured surface morphologies which will be discussed in the subsequent section. The agglomerations of fillers potentially cause a reduction in the nucleation ability of the censopheres leading to increased average size of the spherulites (Fig. 3). The role of filler agglomeration in causing restricted plastic deformation in case of filled elastomers and brittle failure in case of filled thermoplastics is exhaustively reported [21].

The crack opening displacement (COD) has been calculated based on the empirical relationship,

$$w_e = M\sigma_y \mathrm{COD}$$

where σ_y is the yield stress and M is the plastic constrain factor which is taken as 1.15 for DENT specimen [20, 36]. The COD as a function of the cenosphere content is plotted in Fig. 8 and exhibits a similarity in the trend to that of w_e. The COD decreased (like w_e) with the increase in the cenosphere content to 5 wt%, while on increasing the content to 10 wt% the COD sharply decreased and subsequently showed a decreasing trend as the concentration of cenosphere was increased further. Conceptually, COD is a measure of the inherent resistance of the material to stable crack propagation/extension by crack blunting before full-scale initiation (alternatively, COD is related to deformation capacity of the material) and is related to the size of outer plastic deformation zone in the post-yield fracture process zone. The observed local maximum in βw_p at 10 wt% cenosphere which has an inverse correspondence to the COD and direct resemblance to w_e primarily indicates that the crack propagation/extension behaviour in these composites are controlled by the initiation-blunting of the advancing crack in the frontal process zone. The fracture surface morphology, which will be described in detail in the next section, shows

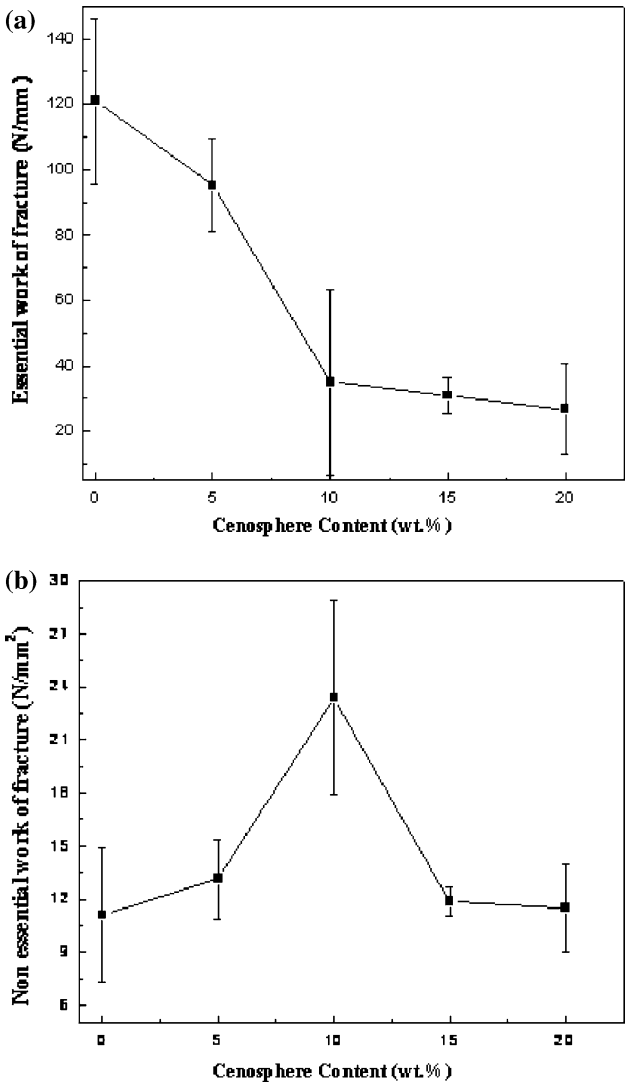

Fig. 6 **a** Variation of essential work of fracture (w_e) as a function of cenosphere loading. **b** Variation of non-essential work of fracture (βw_p) as a function of cenosphere loading

that within the concentration ranging from 5 to 10 wt%, the primary cenosphere (dispersed particles in the as-moulded specimens) particles start forming secondary structures or clusters that entrap polymer chains in the domains closely surrounded by cenosphere particles. The fraction of the polymer domain entrapped amidst closely spaced censopheres undergoes severe plastic deformation under uniaxial tensile loading of the DENT specimens causing viscous flow of the entrapped-polymer phase which gets manifested via fibril-like structures before failure at the microscopic level. Similar dependence of the crack toughness behaviour has also been reported in case of SBR/carbon black-, PVC/$CaCO_3$-, PMMA/silica-, PC/MWNT- and PP/MWNT-based nanocomposites [34, 37–42].

The strong particle–particle interaction and their thermodynamic incompatibility with non-polar PP matrix act as the driving force behind this kind of particle clustering at higher filler concentrations. Such inhomogeneous distribution might also cause high strain localization, which is also attributed to the extreme modulus mismatch between the cenosphere and the PP matrix. Thus, the PP/cenosphere composites within the composition range of 5–10 wt% cenosphere indicate possible composition window in which the polymer-filler interaction builds up, while above 10 wt% cenosphere, two competitive events in the form of polymer–cenosphere and filler–filler interactions become the determinant factors for the crack-resistant behaviour. At a concentration above 10 wt% cenosphere, the filler–filler type network formation is kinetically favoured promoting the cenosphere composites to undergo brittle failure with unstable (high speed) crack propagation, which will be investigated in future by resorting to the evaluation of crack-propagation kinetics. Thus, these composites undergo a double transition, i.e. semiductile-*to*-ductile and ductile-*to*-brittle (together referred as a systematic composition-dependent semiductile-*to*-ductile-*to*-brittle transition) within the investigated composition ranges of 0–10 wt% and 10–30 wt% of cenosphere loadings, respectively. This could be attributed to the fact that up to the critical concentration range (5–10 wt%), the composites undergo preferably plastic deformation as the mechanical deformation is less controlled by the dispersed primary particles. Thus, the different crack toughness behaviour of the composites with varied cenosphere contents may be attributed to the change in cenosphere-induced matrix morphology and filler matrix interactive response.

Fractured surface morphology

The scanning electron microscopic of images of the post-yield fractured surfaces of the selected compositions (with 0, 5, 10, 15 and 20 wt% cenosphere) to enable us study the micro-deformation characteristics before the crack propagation are shown in Fig. 9a–e. The unfilled PP and the composites with 5–10 wt% cenosphere content have primarily been observed to undergo low fracture-strain semiductile-failure accompanied by plastic and shear deformation/flow-induced fibril formation (Fig. 9a–c). The volume of polymer that undergoes yielding determines the total energy absorption and the ultimate mode of fracture in case of filled thermoplastics. The fractured surface micrographs of the composites with cenosphere content below 10 wt% reveal the presence of primary cenosphere particles indicating the absence of any filler-clustering phenomenon. However, the composites with cenosphere content of $\geq$10 wt% show the presence of secondary structures formed by clustering of cenosphere particles. Thus, the large scale plastic flow characteristics as

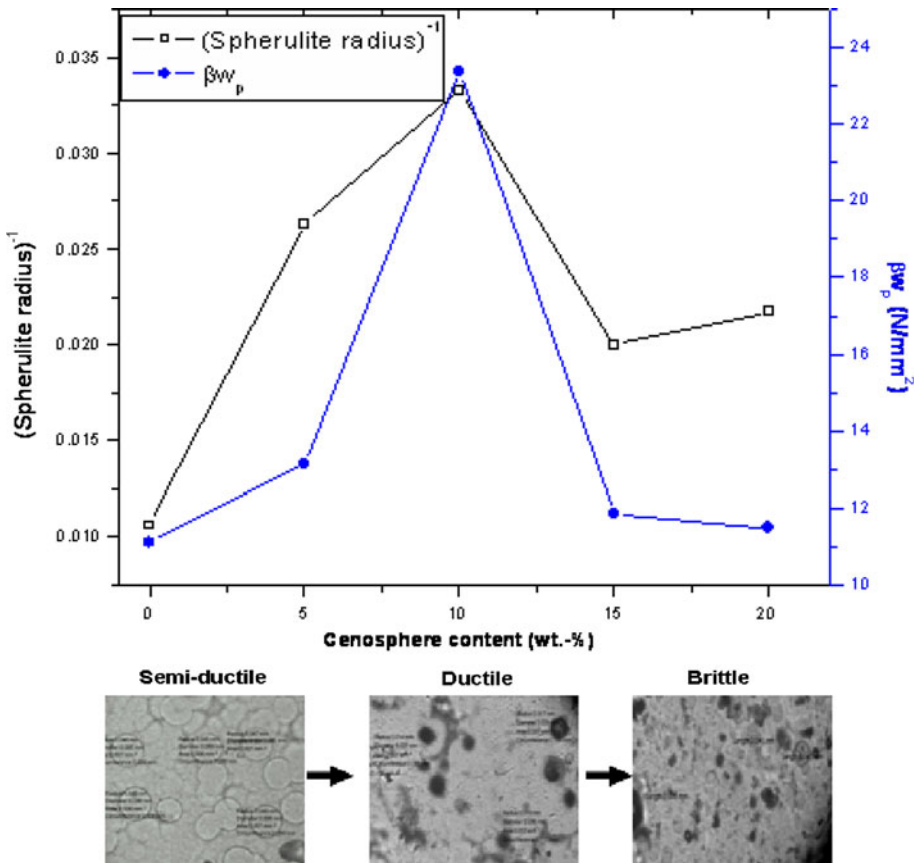

Fig. 7 Morphology-Crack toughness (βw_p) correlation: Dependence of (spherulite radius)$^{-1}$ and βw_p on cenosphere composites

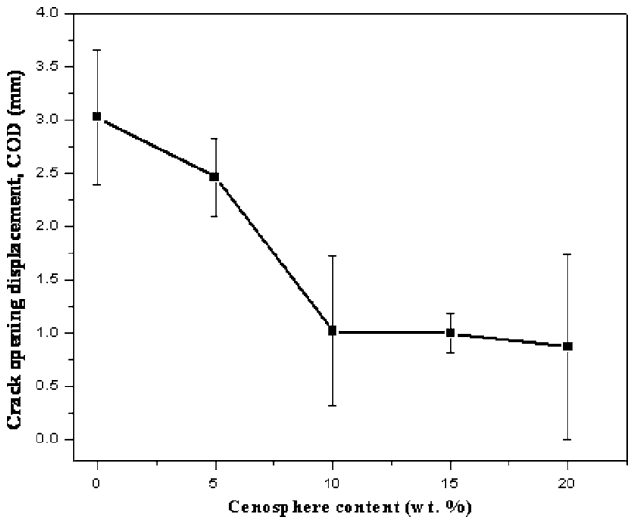

Fig. 8 Variations of crack opening displacement (COD) with cenosphere content

observed in unfilled PP and at low cenosphere concentration are greatly reduced in such composites with cenosphere content of ≥10 wt%. This was clearly revealed from the failure surface topography indicating small-scale yielding of the polymer around the particle clusters shown in Fig. 9c–e. The matrix–cluster interface in the fractured surface contains large number of pullout strands/fibril-like structures of matrix polymer indicating enhanced energy dissipation aided by intrinsic bridging effect (via mechanical restraints posed by the hollow and rigid microspheres) ahead of the frontal crack propagation zone leading to enhanced resistance to crack propagation/toughness maximum in case of the composite with 10 wt% of cenosphere content.

Figure 9d and e show magnified view of such a cluster, where the bridging effect and the presence of large number of micro-voids at the interface are distinctly visible. The formation of micro-voids around the particle clusters facilitates inter-particle matrix yielding, thereby increasing the toughness of filled polymers [42, 43]. Conceptually, the absence of agglomerates/clusters favours multiple yielding which eventually supports the dissipation of the deformation energy and, hence, cause the reduction in the crack growth driving force. This observation of increased toughness in case of the composite with 10 wt% cenosphere content is in agreement with the observed DBT. However, beyond 10 wt% loading of cenosphere, the possibility of filler particles coming closer under uniaxial tension favours agglomeration. In such cases, the crack growth may occur at a much faster pace especially in a scenario of filler agglomerates lying across the crack

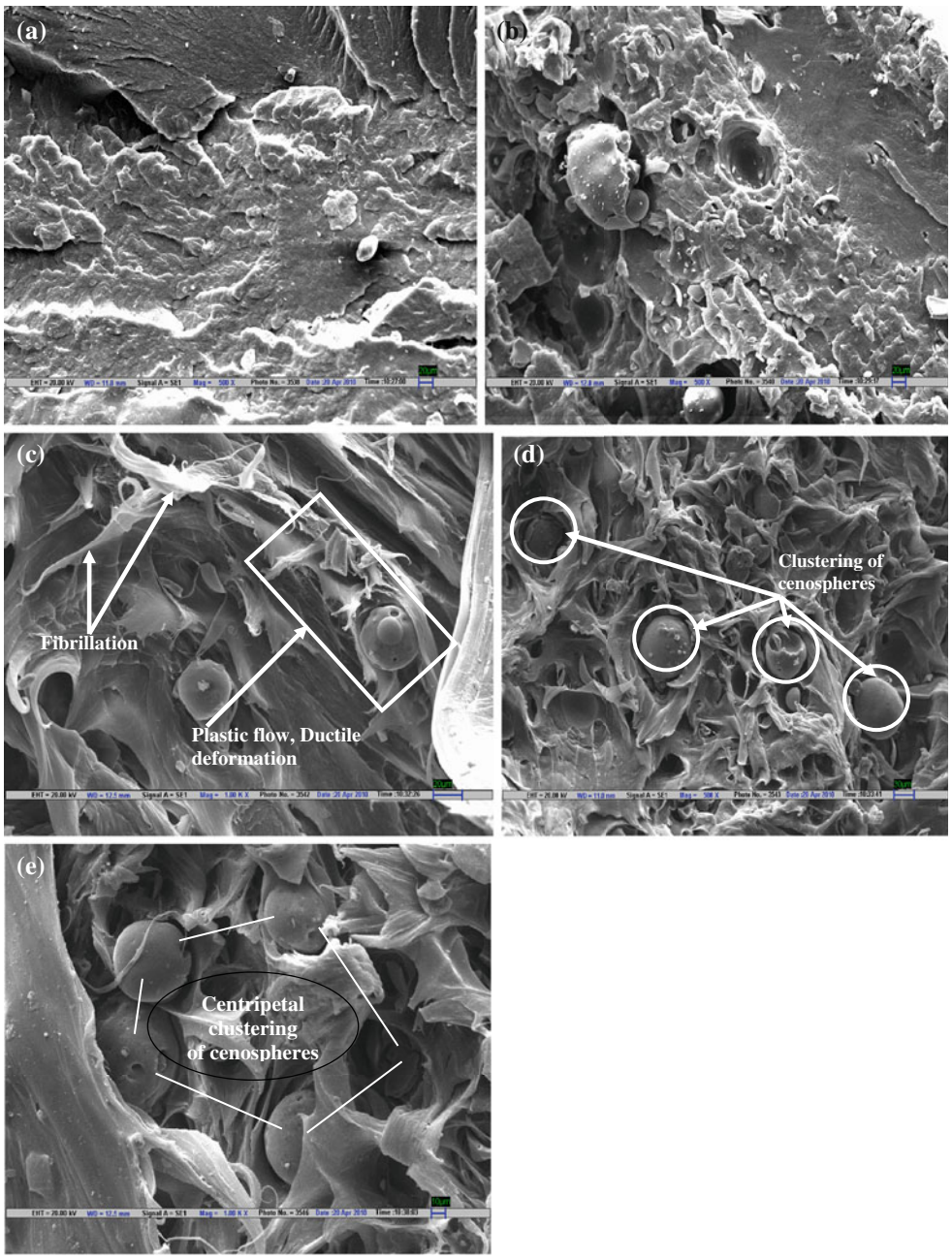

Fig. 9 **a** Fractured surface morphology of PP. **b** Fractured surface morphology of PPC-5. **c** Fractured surface morphology of PPC-10. **d** Fractured surface morphology of PPC-15. **e** Fractured surface morphology of PPC-20

propagation path causing premature low-energy failure i.e. brittle failure mode [44, 45].

Conclusions

Fracture behaviour of cenosphere-filled PP composites is investigated following the essential work of approach (EWF) approach, and the validity of the principles of post yield fracture mechanics (PYFM) preconditions has been confirmed. A maximum in the non-essential work of fracture (NEWF: βw_p) indicating an enhancement in the resistance to crack propagation at 10 wt% of cenosphere content has been observed. A semiductile-*to*-ductile-*to*-brittle transition has been observed in the cenosphere-filled polypropylene (PP) composites, which was adequately supported by the morphological/structural attributes and dynamic mechanical analysis. The transition in the deformation behaviour has also a correspondence with the observed maximum in E'' in thermo-mechanical response to isotropic stress situation. The semiductile-*to*-ductile-*to*-brittle transition is in further agreement with the threefold reduction in the spherulite size in PPC-10 compared to that of PP. The crystallinity has been observed to decrease with

the increase in the cenosphere, and cenosphere as a filler has been found to be α-nucleating. Fractured surface morphology reveals a transition in the failure mode of the composites from matrix-controlled shear deformation mode to filler-controlled quasi-brittle mode above a cenosphere loading of 10 wt% in the composites reiterating the possibility of filler-induced semiductile-*to*-ductile-*to*-brittle transition. Thus, our study conceptually, on one hand, demonstrates the validity of EWF approach to unmodified hollow and rigid-microsphere-filled PP systems as an example for the study of crack toughness behaviour of multicomponent composites with a higher extent of modulus mismatch between the matrix and the reinforcing spherical filler, while on the other hand, it establishes the mechanistic correlations of a systematic semiductile-*to*-ductile-*to*-brittle transition to crystalline morphology (spherulite) dimensions of semicrystalline thermoplastic polymer matrix-filled composites.

Acknowledgements The authors gratefully acknowledge the help extended by Mr. Ratnesh Jain of Micro Minechem India Pvt. Ltd. in providing the flyash-based cenospheres used in this study.

References

1. Fröhlich J, Niedermeier W, Luginsland HD (2005) Compos Part A Appl Sci Manuf 36(4):449
2. Bartczak Z, Argon AS, Cohen RE, Weinberg M (1999) Polymer 40(9):2347
3. Kolay PK, Singh DN (2001) Cement Concrete Res 31(4):539
4. Cardoso RJ, Shukla A, Bose A (2002) J Mater Sci 37:603. doi:10.1023/A:1013781927227
5. Debnath DC, Bandyopadhyaya S, Yu A, Zeng Q, Das T, Blackburn D, White C (2009) J Mater Sci 44:6078. doi:10.1007/s10853-009-3839-3
6. Devi MS, Murugesan V, Rengaraj K, Anand P (1998) J Appl Polym Sci 69:1385
7. Sole BM, Ball A (1996) Tribol Int 29:457
8. Suresha B, Chandramohan G, Siddaramaiah, Jayaraju T (2008) Polym Compos 29(3):307
9. Ramachandra M, Radhakrishna K (2007) Wear 262(11–12):1450
10. Nandan D, Tomar BS, Satapathy BK (2009) Mater Des 30(10):4369
11. Gu J, Wu G, Zhao X (2009) Polym Compos 30(2):232
12. Gu J, Wu G, Zhao X (2008) J Univ Sci Technol Beijing 15:509
13. Gu J, Wu G, Zhang Q (2007) Mater Sci Eng A 452–453:614
14. Jarvela PA, Jarvela PK (1996) J Mater Sci 31:3853. doi:10.1007/BF00352802
15. Murugendrappa MV, Khasim S, Prasad MVNA (2005) Bull Mater Sci 28:565
16. Rohatgi PK, Matsunga T, Gupta N (2009) J Mater Sci 44:1485. doi:10.1007/s10853-008-3165-1
17. Deepthi MV, Sharma M, Sailaja RRN, Anantha P, Sampathkumaran P, Seetharamu M (2010) Mater Des 31:2051
18. Wong KWY, Truss RW (1994) Compos Sci Technol 54:361
19. Tagliavic G, Porfiri M, Gupta N (2010) Compos Part: B Eng 41:86
20. Hashemi S (2003) J Mater Sci 38:3055. doi:10.1023/A:1024752508458
21. Orange E, Bomal Y (2003) Eur Struct Integr Soc 32:39
22. Liang JZ, Li RKY (1999) Polymer 40:3191
23. Orange G (2000) Eur Struct Integr Soc 27:247
24. Gong G, Xie BH, Yang W, Li ZM, Zhang WQ, Yang MB (2005) Polym Testing 24:410
25. Lach R, Schneider K, Weidisch R, Janke A, Knoll K (2005) Eur Polym J 41(2):383
26. Mai YW, Powell P (1991) J Polym Sci Part B Polym Phys 29:785
27. Hill RH (1952) J Mech Phys Solids 1:19
28. Mai YW, Cotterell B (1986) Int J Fracture 32:105
29. Das A, Satapathy BK (2010) Mater Des. doi:10.1016/j.matdes.2010.08.041
30. Wang K, Wu J, Zeng H (2003) Eur Polym J 39:1647
31. Nitta K, Asuka K, Liu B, Terano M (2006) Polymer 47:6457
32. Imai M, Kaji K (2006) Polymer 47:5544
33. Ganß M, Satapathy BK, Thunga M, Weidisch R, Pötschke P, Jehnichen D (2008) Acta Mater 56(10):2247
34. Chen YH, Mai YW, Tong P, Zhang LC (2000) In: Williams JW, Pavan A (eds) Fracture of polymers, composites and adhesion. ESIS Publication, 27. Elsevier, Amsterdam, p 175
35. Arkhireyeva A, Hashemi S, O'Brien M (1999) J Mater Sci 34:5961. doi:10.1023/A:1004776627389
36. Hashemi S, Williams JG (2000) Plast Rubber Compos 29:294
37. Satapathy BK, Weidisch R, Poetschke P, Janke A (2005) Macromol Rapid Commun 26:1246
38. Grellmann W, Caesar T, Heinrich G (1999) Kauts Gummi Kunst 52:37
39. Grellmann W, Heinrich G, Caesar T (2001) In: Grellmann W, Seidler S (eds) Deformation and fracture of polymers. Springer, Berlin, Heidelberg, p 479
40. Reincke K, Lach R, Grellmann W, Heinrich G (2001) In: Grellmann W, Seidler S (eds) Deformation and fracture of polymers. Springer, Berlin, Heidelberg, p 493
41. Lach R, Antonova GL, Grellmann W (2007) Polym Testing 26(1):51
42. Zeng XF, Wang WY, Wang GQ, Chen JF (2008) J Mater Sci 43:3505. doi:10.1007/s10853-008-2475-7
43. Seelig T (2004) On micromechanical modeling of toughening mechanisms and failure in amorphous thermoplastic polymer blends. Vom Fachbereich Mechanik der Technischen Universitat Darmstadt genehmigte Habilitationsschrift
44. Haworth B, Raymond CL, Sutherland I (2001) Polym Eng Sci 41:1345
45. Kinloch AJ, Young RJ (1983) Applied science. London